Change in Electron Configuration of Ferric Ion in Bis(cyanide)(*meso*-tetraalkylporphyrinatoiron(III)), $[Fe(TRP)(CN)_2]^-$, Caused by the Nonplanarity of the Porphyrin Ring

Mikio Nakamura,*[1a] Takahisa Ikeue,[1a] Hiroshi Fujii,*[1b] and Tetsuhiko Yoshimura[1b]

Contribution from the Department of Chemistry, Toho University School of Medicine, Omorinishi, Ota-ku, Tokyo 143, Japan, and Institute for Life Support Technology, Yamagata Technopolis Foundation, Matsuei, Yamagata 990, Japan

Received February 24, 1997[⊗]

Abstract: The synthesis and characterization of a series of bis(cyanide)(*meso*-tetraalkylporphyrinatoiron(III)), $[Fe(TRP)(CN)_2]^-$ where *R* is *H, Me, Et,* and ^iPr, are reported. The ^{1}H NMR spectrum of the unsubstituted $[Fe(THP)(CN)_2]^-$ shows a pyrrole signal at $\delta = -23.19$ ppm (−25 °C) in CD_2Cl_2, which is quite typical as a low spin ferric complex. As the bulkiness of the *meso* substituent increases, the pyrrole signal moves to lower magnetic field; 0.34, −2.26, and 11.94 ppm for $[Fe(TMeP)(CN)_2]^-$, $[Fe(TEtP)(CN)_2]^-$, and $[Fe(T^iPrP)(CN)_2]^-$, respectively. Corresponding to the pyrrole proton signal, the cyanide carbon signal also exhibits a large downfield shift. The difference in chemical shifts between $[Fe(THP)(CN)_2]^-$ and $[Fe(T^iPrP)(CN)_2]^-$ reaches as much as 1443 ppm at −25 °C. The substituent dependent phenomena are also observed in EPR spectra taken in frozen CH_2Cl_2 solution at 4.2 K. While the unsubstituted complex gives a so called large g_{max} type signal at 3.65, the alkyl substituted complexes exhibit axial type spectra; the EPR parameters for $[Fe(T^iPrP)(CN)_2]^-$ are $g_\perp = 2.43$ and $g_\parallel = 1.73$. These results clearly indicate that the electronic ground state changes from the usual $(d_{xy})^2(d_{xz}, d_{yz})^3$ to the unusual $(d_{xz}, d_{yz})^4(d_{xy})^1$ as the substituent becomes bulkier. Analysis of the EPR *g* values reveals that the orbital of the unpaired electron has more than 90% d_{xy} character in the alkyl substituted complexes. The unusual electron configuration is ascribed to the destabilization of d_{xy} orbital and/or stabilization of d_{xz} and d_{yz} orbitals caused by the S_4 ruffled structure of the alkyl substituted porphyrin ring. Thus, in a strongly ruffled low spin complex such as $[Fe(T^iPrP)(L)_2]^\pm$, electron configuration of iron is presented by $(d_{xz}, d_{yz})^4(d_{xy})^1$ regardless of the kind and basicity of the axial ligand (L). In fact, low spin bis(pyridine) complex $[Fe(T^iPrP)(Py)_2]^+$ gives a pyrrole signal at quite a low field, $\delta = +16.4$ ppm at −87 °C, which is actually the lowest pyrrole signal ever reported for the low spin ferric porphyrin complexes. Correspondingly, the EPR spectrum taken at 77 K showed a clear axial type spectrum, $g_\perp = 2.46$ and $g_\parallel = 1.59$. In every case examined, $(d_{xz},d_{yz})^4(d_{xy})^1$ ground state is more or less stabilized by the addition of methanol as exemplified by the further downfield shift of the pyrrole proton and cyanide carbon signals together with the smaller EPR $g_\perp$ values. The methanol effect is explained in terms of the stabilization of d_{xz} and d_{yz} relative to d_{xy} due to the hydrogen bond formation between coordinated cyanide and methanol.

Introduction

Physical and chemical properties of metalloporphyrins are controlled by the electronic configuration of the central metal ions. In fact, various spectroscopic properties such as NMR,[2−5] EPR,[6−9] Mossbauer,[10−12] etc. are affected by it. As for the typical low spin ferric porphyrin complexes where the electron configuration is presented by $(d_{xy})^2(d_{xz}, d_{yz})^3$, characteristics of the NMR and EPR spectra have been well documented. Examples are bis(imidazole) and bis(cyanide) complexes of tetraarylporphyrinatoiron(III).[13,14] ^{1}H NMR signals for the pyrrole β-protons in these complexes appear at extremely high magnetic field, δ −20 to −30 ppm at −60 °C. Large upfield shift of the pyrrole β-protons indicates the existence of large spin densities on the pyrrole β-carbons, which is induced by the interactions between porphyrin (p_π) and iron (d_π) orbitals. Among them, the major interaction is assigned to the one between occupied porphyrin $3e_g$ and singly occupied iron d_π (d_{xz} or d_{yz}) orbitals.[2] Since the $3e_g$ orbital places large electron

⊗ Abstract published in *Advance ACS Abstracts,* June 15, 1997.

(1) (a) Toho University School of Medicine. (b) Institute for Life Support Technology.

(2) La Mar, G. N.; Walker, F. A. In *The Porphyrins, Vol. IV*; Dolphin, D., Ed.; Academic Press: New York, 1979; pp 61−157.

(3) Vertini, I; Luchinat, C. In *NMR of Paramgnetic Molecules in Biological Systems*, Lever, A. B. P., Gray, H. B., Eds.; The Benjamin/Cummings: Menlo Park, CA, 1986; pp 165−229.

(4) Vertini, I; Luchinat, C. In *NMR of Paramagnetic Substances, Coordination Chemistry* Reviews; Lever, A. B. P., Ed.; Elsevier: Amsterdom, 1996; p 292.

(5) Goff, H. M. In *Iron Porphyrin, Part One*; Lever, A. B. P., Gray, H. B. Eds.; The Benjamin/Cummings: Menlo Park, CA, 1983; pp 45−88.

(6) Palmer, G. In *Iron Porphyrin, Part Two*; Lever, A. B. P., Gray, H. B., Eds.; The Benjamin/Cummings: Menlo Park, CA, 1983; pp 237−281.

(7) Walker, F. A.; Reis, D.; Balke, V. L. *J. Am. Chem. Soc.* **1984**, *106*, 6888−3898.

(8) Walker, F. A.; Huynh, B. H.; Scheidt, W. R.; Osvath, S. R. *J. Am. Chem. Soc.* **1986**, *108*, 5288−5297.

(9) Safo, M. K.; Gupta, G. P.; Walker, F. A.; Scheidt, W. R. *J. Am. Chem. Soc.* **1991**, *113*, 5497−5510.

(10) Sams, J. R.; Tsin, T. B. In *The Porphyrins, Vol. IV*; Dolphin, D., Ed.; Academic Press: New York, 1979; pp 425−478.

(11) Medhi, O. K.; Silver, J. *J. Chem. Soc., Dalton Trans.* **1990**, 555−559.

(12) Marsh, P. J.; Silver, J.; Symons, M. C.; Taiwo, F. A. *J. Chem. Soc., Dalton Trans.* **1996**, 2361−2369.

(13) Nakamura, M.; Tajima, K.; Tada, K.; Ishizu, K.; Nakamura, N. *Inorg. Chim. Acta* **1994**, *224*, 113−124.

(14) La Mar, G. N.; Gaudio, J. D.; Frye, J. S.; *Biochim. Biophys. Acta* **1977**, *498*, 422−435.

S0002-7863(97)00602-1 CCC: $14.00

densities on the pyrrole β-carbons, the spin transfer from porphyrin ($3e_g$) to iron (d_π) results in the large spin densities on these carbons, which would be translated as a large upfield shift of the pyrrole β-protons. EPR spectra of these complexes also give characteristic signals that are classified into two types depending on the kind and orientation of the axial ligands: (i) rhombic spectrum in which three signals are observed at g = 2.8−2.9, 2.2−2.4, and 1.5−1.6 and (ii) a large g_{max} type spectrum in which one resolved signal appears at $g > 3.4$.[8]

Recent NMR studies have revealed, however, that some low spin ferric porphyrin complexes give pyrrole signals at unusually low magnetic field.[15−23] Examples are bis(*tert*-butyl isocyanide)(tetraphenylporphyrinatoiron(III)) [Fe(TPP)(^{t}BuNC)$_2$]$^+$,[15,23] bis(4-cyanopyridine)(tetramesitylporphyrinatoiron(III)) [Fe(TMP)(4-CNPy)$_2$]$^+$,[17] and bis(dimethylphenylphosphonite)(tetraphenylporphyrinatoiron(III)) [Fe(TPP){P(OMe)$_2$Ph}$_2$]$^+$,[19] where pyrrole signals were observed at δ 9.73 (25 °C), 2.1 (−80 °C), and 2.56 (25 °C) ppm, respectively. In addition to the low field pyrrole shift, *meta*-protons of the *meso* aryl groups also appeared at rather low field. These complexes commonly possess axial ligands with weak σ donating and strong π accepting ability. Walker and the co-workers have shown based on the NMR, EPR, Mossbauer, and MCD spectra that the electronic ground state of [Fe(TMP)(4-CNPy)$_2$]$^+$ and [Fe(TPP)(4-CNPy)$_2$]$^+$ is largely $(d_{xz}, d_{yz})^4(d_{xy})^1$ in contrast to the usual $(d_{xy})^2(d_{xz}, d_{yz})^3$.[17,20,21] The unusual electronic ground state was ascribed to the stabilization of d_{xz} and d_{yz} orbitals of iron by the interaction with relatively low lying π* orbitals of the axial ligands. Simonneaux and co-workers[19] also ascribed the low field pyrrole signal in [Fe(TPP){P(OMe)$_2$Ph}$_2$]$^+$ to the low basicity of the phosphonite ligand.

Some years ago, we reported the existence of the unusually low field pyrrole signals in the low spin bis(2-methylbenzimidazole) complex [Fe(TMP)(2-MeBzIm)$_2$]$^+$.[16] This complex gave four pyrrole signals due to the hindered rotation of the coordinated 2-MeBzIm in the range of 0.1−1.2 ppm at −58 °C. The EPR spectrum of this complex taken at 4.5 K in frozen CH_2Cl_2 solution showed axial signal at $g_\perp = 2.61$, which is quite close to $g_\perp = 2.53$ (77 K) of [Fe(TMP)(4-CNPy)$_2$]$^+$ and $g_\perp = 2.365$ (90 K) of [Fe(TPP){P(OMe)$_2$Ph}$_2$]$^+$. The complex has relatively large spin densities on the *meso* carbons as exemplified by the unusually low chemical shifts of the *meso* carbons and *meso* aromatic protons; the *meso* carbon signal appeared at 321 ppm at −51 °C, and the mesityl *meta* proton signals were observed at 10.5 to 11.0 ppm at −58 °C. Similarity of the NMR and EPR spectral properties of this complex to those of [Fe(TMP)(4-CNPy)$_2$]$^+$,[17] [Fe(TPP){P(OMe)$_2$Ph}$_2$]$^+$,[19] and [Fe(TPP)(^{t}BuNC)$_2$]$^+$ [15,23] might be the suggestion that the electron configuration of this complex is also presented by $(d_{xz}, d_{yz})^4(d_{xy})^1$. The only difference is that the basicity of 2-MeBzIm is much higher than those of the other three.

Recently, we have encountered quite novel complexes with unusually low pyrrole signals in a series of bis(2-methylimidazole)(tetraalkylporphyrinatoiron(III)) [Fe(T*R*P)(2-MeIm)$_2$]$^+$ where *R* = *Me*, *Et*, and ^{i}*Pr*.[22] Particularly interesting are the pyrrole signals of the isopropyl complex [Fe(T^i*Pr*P)(2-MeIm)$_2$]$^+$. All four signals appeared at so called *diamagnetic region*, 3.2, 4.3, 7.4, and 7.8 ppm. Although the NMR spectral properties of this complex are similar to those of [Fe(TMP)(4-CNPy)$_2$]$^+$, [Fe(TPP){P(OMe)$_2$Ph}$_2$]$^+$, and [Fe(TPP)(^{t}BuNC)$_2$]$^+$, the basicities of the axial ligands are greatly different; the K_b value of 2-MeIm is larger than that of 4-CNPy by 10^6! As the bulkiness of the *meso* substituents decreases, the pyrrole signal moved to the normal region. Thus, [Fe(T*Me*P)(2-MeIm)$_2$]$^+$ and [Fe(T*Et*P)(2-MeIm)$_2$]$^+$ showed pyrrole signals at −8.2 and −9.4 ppm, respectively, at −35 °C, and the unsubstituted [Fe(T*H*P)(2-MeIm)$_2$]$^+$ showed it at quite a normal position, −21.7 ppm. Therefore, it might be difficult to ascribe the reason for the low field pyrrole shifts in these complexes to the basicity or the energy level of the π* orbital of the axial ligand.

Recent X-ray crystallographic results of tetraisopropylporphyrinatonickel(II) [Ni(T^i*Pr*P)] have revealed that the complex is highly ruffled due to the severe steric repulsion between *meso*-isopropyl groups and pyrrole β-hydrogens.[24] In contrast, the porphyrin ring of the methyl analogue [Ni(T*Me*P)] was reported to be slightly nonplanar[25−27] and that of unsubstituted [Ni(T*H*P)] was recently proved to be planar.[28] Thus, the pyrrole shifts in [Fe(T*R*P)(2-MeIm)$_2$]$^+$ correlate well with the nonplanarity of the porphyrin ring. Based on these results, we have explained that the unusually low pyrrole shifts especially in the isopropyl complex [Fe(T^i*Pr*P)(2-MeIm)$_2$]$^+$ is caused by the strongly ruffled porphyrin ring; ring deformation would deteriorate the iron(dπ)−porphyrin(pπ) overlaps and decrease the spin densities on the pyrrole carbons.[22] The above results could be explained, however, in a different way; the increased deformation of the porphyrin ring varies the electron configuration of iron from the usual $(d_{xy})^2(d_{xz}, d_{yz})^3$ to the unusual $(d_{xz}, d_{yz})^4(d_{xy})^1$ in spite of the coordination of a relatively strong base. Elucidation of the relationship between porphyrin nonplanarity and electron configuration of iron is quite important since the crystallographic studies of heme proteins have revealed that the hemes in protein cavities are in some cases nonplanar.[29−31] Although effects of nonplanar porphyrin ring on the physicochemical properties of the complex have been extensively studied, including spectroscopic[32−39] and redox properties,[40−43] there have been

(15) Simonneaux, G; Hindre, F.; Le Olouzennec, M. *Inorg. Chem.* **1989**, *28*, 823−825.
(16) Nakamura, M.; Nakamura, N. *Chem. Lett.* **1991**, 1885−1888.
(17) Safo, M. K.; Gupta, G. P.; Watson, C. T.; Simonis, U.; Walker, F. A.; Scheidt, W. R. *J. Am. Chem. Soc.* **1992**, *114*, 7066−7075.
(18) Geze, C.; Legrand, N.; Bondon, A.; Simonneaux G. *Inorg. Chim. Acta* **1992**, *195*, 73−76.
(19) Guillemot, M.; Simonneaux G. *J. Chem. Soc., Chem. Commun.* **1995**, 2093−2094.
(20) Safo, M. K.; Walker, F. A.; Raitsimring, A. M.; Walters, W. P.; Dolata, D. P.; Debrunner, P. G.; Scheidt, W. R. *J. Am. Chem. Soc.* **1994**, *116*, 7760−7770.
(21) Cheesman, M. R.; Walker, F. A. *J. Am. Chem. Soc.* **1996**, *118*, 7373−7380.
(22) Nakamura, M.; Ikeue, T.; Neya, S.; Funasaki, N.; Nakamura, N. *Inorg. Chem.* **1996**, *35*, 3731−3732.
(23) Walker, F. A.; Nasri, H.; Turowska-Tyrk, I.; Mohanrao, K.; Watson, C. T.; Shokhirev, N. V.; Debrunner, P. G.; Scheidt, W. R. *J. Am. Chem. Soc.* **1996**, *118*, 12109−12118.
(24) Ema, T.; Senge, M. O.; Nelson, N. Y.; Ogoshi, H.; Smith, K. M. A*ngew. Chem., Int. Ed. Engl.* **1994**, *33*, 1879−1881.
(25) Gallucci, J. C.; Swepston, P. N.; Ibers, J. A. *Acta Crystallogr.* **1982**, *38*, 2134.
(26) Kutzler, F. W.; Swepston, P. N.; Yellin, Z. B.; Ellis, D. E.; Ibers, J. A. *J. Am. Chem. Soc.* **1983**, *105*, 2996−3004.
(27) Newcomb, T. P.; Godfrey, M. R.; Hoffman, B. M.; Ibers, J. A. *J. Am. Chem. Soc.* **1989**, *111*, 7078−7084.
(28) Jantzen, W.; Tyrk, I. T.; Scheidt, W. R.; Schelnutt, J. A. *Abstract of 210th ACS National Meeting*; Inorg. Division, 531. August, 1995.
(29) Hobbs, J. D.; Schelnutt, J. A. *J. Protein Chem.* **1995**, *14*, 19−25.
(30) Louie, G. V.; Brayer, G. D. *J. Mol. Biol.* **1990**, *212*, 527−555.
(31) Berghuis, A. M.; Brayer, G. D. *J. Mol. Biol.* **1992**, *214*, 959−976.
(32) Senge, M. O.; Ema, T.; Smith, K. M. *J. Chem. Soc., Chem. Commun.* **1995**, 733−734.
(33) Takeda, J.; Sato, M. *Chem. Lett.* **1995**, 971−972.
(34) Sparks, L. D.; Anderson, K. K.; Medforth, C. J.; Smith, K. M.; Shelnutt, J. A. *Inorg. Chem.* **1994**, *33*, 2297−2302.
(35) Piffat, C.; Melamed, D.; Spiro, T. G. *J. Phys. Chem.* **1993**, *97*, 7441.
(36) Lin, C. Y.; Hu, S.; Rush III, T.; Spiro, T. G. *J. Am. Chem. Soc.* **1996**, *118*, 9452−9453.
(37) Hobbs, J. D.; Majumder, S. A.; Luo, L.; Sickelsmith, G. A.; Quirke, J. M. E.; Medforth, C. J.; Smith, K. M.; Shelnutt, J. A. *J. Am. Chem. Soc.* **1994**, *116*, 3261−3270.

Chart 1

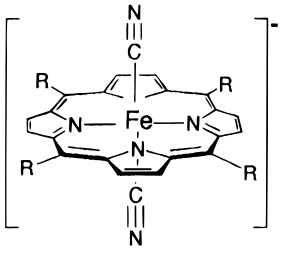

[Fe(TRP)(CN)$_2$]$^-$Bu$_4$N$^+$

R = H, Me, Et, ^{i}Pr

few systematic studies on the relationship between electron configuration of iron and the nonplanarity of the porphyrin ring.[20] In order to clarify the relationship, we have measured ^{1}H NMR, ^{13}C NMR, and EPR spectra of a series of bis(cyanide)-(*meso*-tetraalkylporphyrinatoiron(III)) complexes, [Fe(T*R*P)-(CN)$_2$]$^-$ where *R* = *H*, *Me*, *Et*, and ^{i}*Pr*, and have tried to determine if the electron configuration of iron changes due to the nonplanarity of the porphyrin ring. We have chosen the bis(cyanide) complexes by the following reasons. (1) Cyanide is a typical ligand to form a low spin ferric complex.[14,44] (2) Coordinated cyanide is considered to be a good proton acceptor in hydroxylic solvent such as methanol.[14] Thus, it might be possible to obtain two sets of spectroscopic data by using two solvent systems, CD_2Cl_2 and $CD_2Cl_2-CD_3OD$, in which cyanide behaves as an axial ligand with different coordination strength. (3) ^{13}C Chemical shifts of the coordinated cyanide ligand could give valuable information on the electron configuration since it is directly bonded to the ferric ion. In this paper, we would like to report that the electron configuration of iron in low spin [Fe(T*R*P)(CN)$_2$]$^-$ complexes does change as the porphyrin ring goes from planar to nonplanar structure.

Experimental Section

General Methods. Pyrrole, acetaldehyde, propionaldehyde, isobutylaldehyde, and pyridine were purchased from Aldrich, and they were distilled before use. Formalin, 37% solution in water, was also purchased from Aldrich and was used without further purification. ^{1}H and ^{13}C NMR spectra were recorded either on a JEOL JNM-620 operating at 620 MHz for proton or on a JEOL FX90Q operating at 90 MHz. Chemical shifts were referenced to residual $CHDCl_2$ ($\delta = 5.32$ ppm for ^{1}H and 54.2 ppm for ^{13}C). EPR spectra were measured at 77 and 4.2 K with a Brucker ESP-300 spectrometer operating at X band and equipped with an Oxford helium cryostat.

Synthesis of [Fe(T*H*P)]Cl. Synthesis of the free base porphine was carried out according to Neya's method.[45] A solution containing propionic acid (500 mL) and pyridine (5 mL) was heated to 90 °C. To this solution, 0.9 mL (13 mmol) of freshly distilled pyrrole and 0.9 mL of formalin (12 mmol) were added at 10 min interval. After total addition of 7.2 mL of pyrrole (104 mmol) and 7.2 mL of formalin (96 mmol), the solution was heated for further 1 h at this temperature followed by bubbling air into the hot solution over 5 min. To the cooled solution was added 200 mL of chloroform, and the mixture was washed with water (200 mL × 2), 0.1 M NaOH (250 mL × 2), and then with water (300 mL) to separate propionic acid. The chloroform layer was dried over sodium sulfate, treated with *p*-chloranil (1.0 g) at 62 °C for 1 h, and purified by the chromatography on silica gel. Elution with CH_2Cl_2 gave 50 mg of the pure product. Insertion of iron was performed as follows. The pure porphine (50 mg), sodium acetate (7.5 mg), and $FeCl_2 \cdot 6H_2O$ (50 mg) were dissolved in acetic acid (30 mL), and the solution was refluxed for 90 min. After the solution was cooled, diluted HCl was added. The mixture was extracted with $CHCl_3$, and the organic layer was dried over sodium sulfate. After the evaporation of the solvent, the high spin [Fe(T*H*P)]Cl thus formed was separated by chromatography on silica gel using $CH_2Cl_2-CH_3OH$ as the eluent and recrystallized from CH_2Cl_2−hexane to yield 60 mg (92%) of the pure material. ^{1}H NMR ($CDCl_3$, δ) 77.9 (pyrrole-H), −62.3 (*meso*-H).

Synthesis of [Fe(T*Me*P)]Cl.[46] In a 1 L flask equipped with reflux condenser, thermometer, and magnetic bar were placed 4.07 g of pyrrole (61 mmol), 0.87 g of acetaldehyde (20 mmol), and 300 mL of propionic acid containing 12 mL of water and 1 mL of pyridine. The solution was heated at 85 °C and stirred for 2 h. The reaction mixture was cooled and treated similarly as in the case of porphine. The yield was 160 mg (8.7%). Insertion of iron followed by the purification as in the case of [Fe(T*H*P)]Cl yielded 179 mg (90%) of the pure complex. ^{1}H NMR ($CDCl_3$, δ) 87.6(pyrrole-H), 127.6 (*meso*-CH3).

Synthesis of [Fe(T*Et*P)]Cl.[46] (T*Et*P)H2 was prepared from pyrrole (61 mmol) and propionaldehyde(29 mmol) in propionic acid containing 12 mL of water and 1 mL of pyridine at 90 °C. The yield was 188 mg (6.1%). Insertion of iron followed by the purification as in the case of [Fe(T*H*P)]Cl gave the pure complex in 88% yield. ^{1}H NMR($CDCl_3$, δ) 88.6 (pyrrole-H), 62.1 (meso -CH_2CH$_3$), 7.2 (*meso*-CH$_2$CH_3).

Synthesis of [Fe(T^i*Pr*P)]Cl. (T^i*Pr*P)H$_2$ was prepared from pyrrole (61 mmol) and isobutylaldehyde (44 mmol) in propionic acid in 368 mg (7.0%) yield. Insertion of iron followed by the purification as in the case of [Fe(T*H*P)]Cl gave the pure complex in 30% yield. ^{1}H NMR ($CDCl_3$, δ) 90.5 (pyrrole-H), 28.9 (*meso*-C*H*(CH$_3$)$_2$), 9.5 (*meso*-CH-(CH_3)$_2$).

Synthesis of Bis(cyanide) Complexes. Bis(cyanide) complex, [Fe(T*R*P)(CN)$_2$]$^-$, was prepared in an NMR sample tube by the two different methods. Method A: To a 250 μL CD_2Cl_2 solution containing 1.0−1.2 mg of [Fe(T*R*P)]Cl was added a CD_3OD solution (25 μL, 3.0 mol equiv) of KCN. Formation of the low spin [Fe(T*R*P)(CN)$_2$]$^-$K$^+$ was confirmed by the disappearance of the pyrrole signal of the starting high spin complex at an extremely low field. Method B: To a 250 μL of CD_2Cl_2 containing 1.0−1.2 mg of [Fe(T*R*P)]Cl was added a CD_2Cl_2 solution (25 μL, 3.0 mol equiv) of tetrabutylammonium cyanide. Formation of [Fe(T*R*P)(CN)$_2$]$^-$Bu$_4$N$^+$ was confirmed similarly.

Synthesis of Bis(cyanide) Complexes with ^{13}C Enriched Cyanide. Potassium cyanide, K^{13}CN (99% ^{13}C), was purchased from ISOTEC and was used to obtain [Fe(T*R*P)(^{13}CN)$_2$]$^-$K$^+$ by method A. Tetrabutylammonium cyanide, Bu4N^{13}CN, was prepared from K^{13}CN and Bu$_4$-NCl in THF−MeOH. After the removal of the precipitated KCl, the solution was evaporated to dryness. The oily Bu$_4$N^{13}CN thus formed was dried in a vacuum and used to prepare [Fe(T*R*P)(^{13}CN)$_2$]$^-$Bu$_4$N$^+$ by method B.

Results

Spectral Properties in Dichloromethane Solution. (i) ^{1}H NMR Spectra. The ^{1}H NMR spectra of a series of [Fe-(T*R*P)(CN)$_2$]$^-$Bu$_4$N$^+$ in CD_2Cl_2 were taken over a wide temperature range, +25 to −80 °C. Example spectra at 25 °C are shown in Figure 1. In Table 1 are listed the chemical shifts at −25 °C. As is clear from the data in Table 1, the pyrrole signals showed drastic change depending on the *meso* substituents. While the pyrrole signal for [Fe(T*H*P)(CN)$_2$]$^-$Bu$_4$N$^+$ appeared at a normal position as a low spin complex, −23.19 ppm, those for [Fe(T*Me*P)(CN)$_2$]$^-$Bu$_4$N$^+$ and [Fe(T*Et*P)(CN)$_2$]$^-$Bu$_4$N$^+$ were observed at much lower field, 0.34 and −2.26 ppm, respectively.

(38) Medforth, C. J.; Muzzi, C. M.; Smith, K. M.; Abraham, R. J.; Hobbs, J. D.; Schelnutt, J. A. *J. Chem. Soc., Chem. Commun.* **1994**, 1843−1844.
(39) Nakamura, M. *Bull. Chem. Soc. Jpn.* **1995**, *68*, 197−203.
(40) Hariprasad, G.; Dahal, S.; Maiya, B. G. *J. Chem. Soc. Dalton Trans.* **1996**, 3429−3436.
(41) Tagliatesta, P.; Li, J.; Autret, M.; Caemelbecke, E. V.; Villard, A.; D'Souza, F.; Kadish, K. M. *Inorg. Chem.* **1996**, *35*, 5570−5576.
(42) Hodge, J. A.; Hill, M. G.; Gray, H. B. *Inorg. Chem.* **1995**, *34*, 809−812.
(43) Ravikanth, M.; Reddy, D.; Mirsa, A.; Chandrashekar, T. K. *J. Chem. Soc., Dalton Trans.* **1993**, 1137−1141
(44) Wang, J. T.; Yeh, H. J. C.; Johnson, D. F. *J. Am. Chem. Soc.* **1978**, *100*, 2400−2405.
(45) Neya, S.; Yodo, H.; Funasaki, N. *J. Heterocyclic Chem.* **1993**, *30*, 549−550.
(46) Neya, S; Funasaki, N. *J. Heterocyclic Chem.* **1997**, *34*, 689−690.

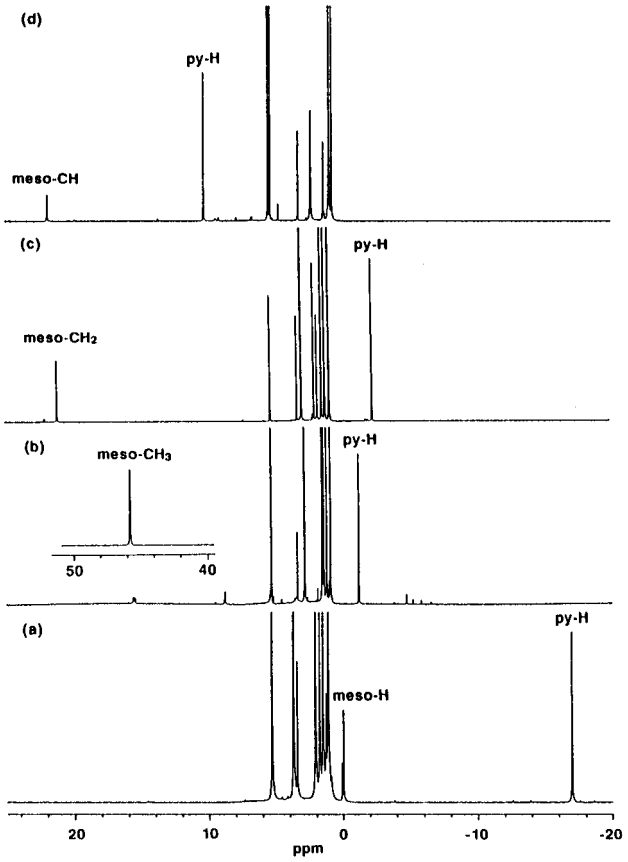

Figure 1. ^{1}H NMR spectra (620 MHz) of a series of [Fe(T*R*P)-(CN)$_2$]$^-$Bu$_4$N$^+$ taken at 25 °C in CD_2Cl_2: (a) $R = H$, (b) $R = Me$, (c) $R = Et$, and (d) $R = {}^iPr$.

Table 1. ^{1}H NMR Chemical Shifts of [Fe(T*R*P)(CN)$_2$]$^-$Bu$_4$N$^+$ at −25 °C in CD_2Cl_2 and CD_2Cl_2−CD_3OD (γ ppm)

	CD_2Cl_2			CD_2Cl_2−CD_3OD		
R	Py-H[a]	α-H[b]	*β*-H[c]	Py-H	α-H	*β*-H
H	−23.19	(−2.99)[d]		−21.73	(0.03)[d]	
Me	0.34	64.21		8.65	99.05	
Et	−2.26	27.54	2.51	8.27	48.43	4.71
^{i}*Pr*	11.94	26.93	6.45	12.76	29.69	6.84

[a] Pyrrole protons. [b] *meso*-α-Protons. [c] *meso*-*β*-Protons. [d] Chemical shifts of the protons directly bonded to the *meso*-carbons.

In the case of [Fe(T^i*Pr*P)(CN)$_2$]$^-$Bu$_4$N$^+$, the pyrrole signal shifted to 11.94 ppm.

(ii) ^{13}C NMR Spectra. The ^{13}C NMR signals of the coordinated cyanide in a series of [Fe(T*R*P)(^{13}CN)$_2$]$^-$Bu$_4$N$^+$ were observed at 25 °C and −25 °C in CD_2Cl_2. Example spectra at 25 °C are shown in Figure 2. In Table 2 are listed the chemical shifts at −25 °C. As is clear from the data, the cyanide signal moved to lower magnetic field as the bulkiness of the *meso* substituents increases; the chemical shifts of the cyanide signals of [Fe(T*H*P)(CN)$_2$]$^-$Bu$_4$N$^+$ and Fe-(T*iPr*P)(CN)$_2$]$^-$Bu$_4$N$^+$ were −2541 and −1347 ppm, respectively, at 25 °C.

(iii) EPR Spectra. EPR spectra were obtained at 77 and 4.2 K in frozen CH_2Cl_2 solution. While the unsubstituted [Fe(T*H*P)(CN)$_2$]$^-$Bu$_4$N$^+$ gave no signal at 77 K, [Fe(T*Me*P)-(CN)$_2$]$^-$Bu$_4$N$^+$ and [Fe(T*Et*P)(CN)$_2$]$^-$Bu$_4$N$^+$ showed very broad signals at ca. $g = 2.4$. In the case of the isopropyl complex [Fe(T^i*Pr*P)(CN)$_2$]$^-$Bu$_4$N$^+$, however, an axial type spectrum with sharp line width was observed at $g_\perp = 2.4$ and $g_\parallel = 1.7$. Much clearer signals were observed when the EPR spectra were taken at 4.2 K. As shown in Figure 3, the unsubstituted complex

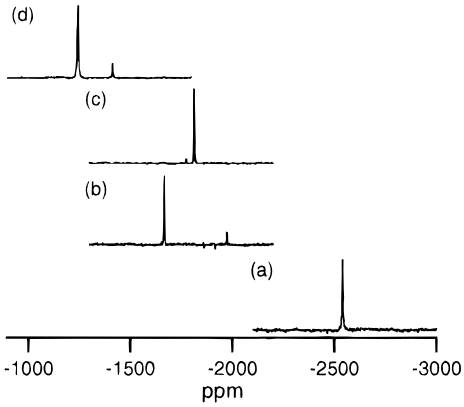

Figure 2. ^{13}C NMR spectra (156 MHz) of a series of [Fe(T*R*P)-(CN)$_2$]$^-$Bu$_4$N$^+$ taken at 25 °C in CD_2Cl_2: (a) $R = H$, (b) $R = Me$, (c) $R = Et$, and (d) $R = {}^iPr$.

Table 2. ^{13}C NMR Chemical Shifts of the Coordinated Cyanide in a Series of [Fe(T*R*P)(CN)$_2$]$^-$Bu$_4$N$^+$ Complexes at −25 °C in CD_2Cl_2 and in CD_2Cl_2−CD_3OD (δ ppm)

R	CD_2Cl_2	CD_2Cl_2−CD_3OD	$\Delta\delta$[a]
H	−2973	−2963	10
Me	−1840	−1401	439
Et	−2054	−1557	497
^{i}*Pr*	−1530	−1389	141

[a] Difference in chemical shifts between two solvent systems.

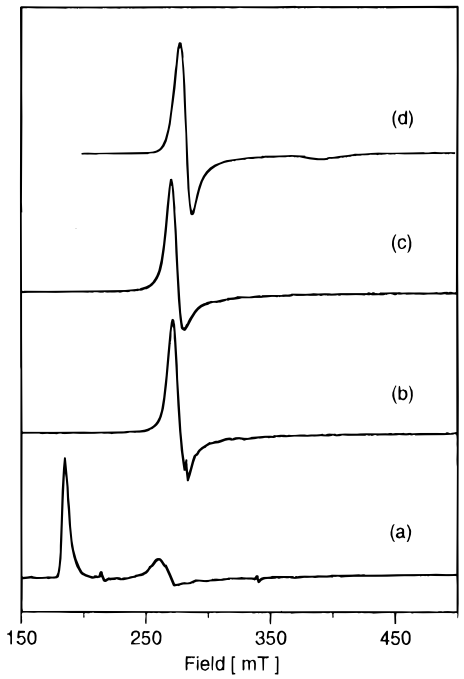

Figure 3. EPR spectra of a series of [Fe(T*R*P)(CN)$_2$]$^-$Bu$_4$N$^+$ taken at 4.2 K in frozen CH_2Cl_2 solution: (a) $R = H$, (b) $R = Me$, (c) $R = Et$, and (d) $R = {}^iPr$.

showed a so called large g_{max} signal at 3.65. All of the alkyl substituted complexes, however, gave axial type spectra. In Table 3 are listed the EPR g values obtained at 4.2 K.

Spectral Properties in Dichloromethane−Methanol Solution. The ^{1}H NMR, ^{13}C NMR, and EPR spectra of these complexes changed to a great extent in the presence of methanol.

(i) ^{1}H NMR Spectra. The ^{1}H NMR spectra for a series of [Fe(T*R*P)(CN)$_2$]$^-$Bu$_4$N$^+$ were taken in CD_2Cl_2 in the presence of 10 volume % of CD_3OD. The results were also given in Table 1. These data indicate that some of the signals showed considerably large low field shifts in the presence of methanol;

Table 3. EPR Parameters and Coefficients[a] of a Series of $[Fe(TRP)(CN)_2]^-Bu_4N^+$ Complexes at 4.2 K

	CH_2Cl_2			$CH_2Cl_2-CH_3OH$					
R	$\|g_x\|$	$\|g_y\|$	$\|g_z\|$	$\|g_x\|$	$\|g_y\|$	$\|g_z\|$	*a*	*b*	*c*
H			3.65			3.5			
Me	2.46	2.46		2.43	2.43	1.69	0.147	0.147	0.965
Et	2.48	2.48		2.47	2.47	1.61	0.167	0.167	0.957
^{i}Pr	2.43	2.43	1.73	2.35	2.35	1.82	0.110	0.110	0.979

[a] The coefficients *a*, *b*, and *c* are those of the wave functions for d_{xz}, *dyz*, and *dxy*, respectively.

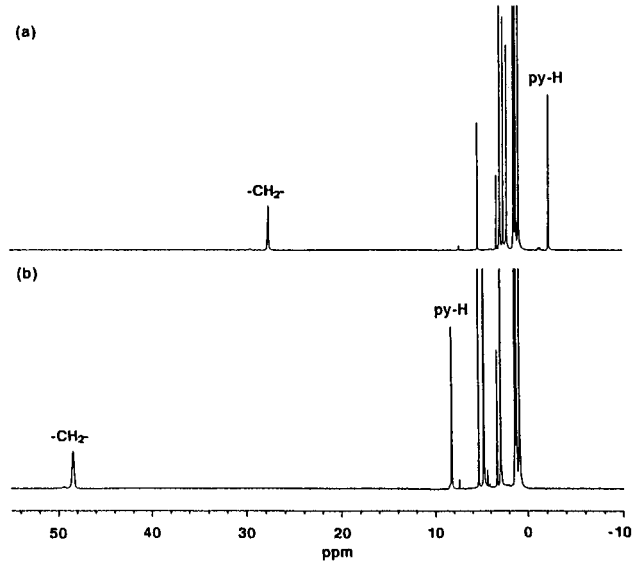

Figure 4. ^1H NMR spectra (620 MHz) of $[Fe(TEtP)(CN)_2]^-Bu_4N^+$ taken at −25 °C in (a) CD_2Cl_2 and (b) $CD_2Cl_2-CD_3OD$.

the low field shifts of the pyrrole protons in $[Fe(TMeP)(CN)_2]^-Bu_4N^+$ and $[Fe(TEtP)(CN)_2]^-Bu_4N^+$ reached as much as 8−10 ppm. In contrast, shifts were much smaller in $[Fe(THP)(CN)_2]^-Bu_4N^+$ and $[Fe(T^iPr\ P)(CN)_2]^-Bu_4N^+$, 1.46 and 0.82 ppm, respectively. The large low field shifts were also obvious in the α-protons of the *meso* substituents. Thus, the methyl signal in $[Fe(TMeP)(CN)_2]^-Bu_4N^+$ moved from 64.21 to 99.05 ppm, and the methylene signal in $[Fe(TEtP)(CN)_2]^-Bu_4N^+$ shifted from 27.54 to 48.43 ppm. In the case of $[Fe(T^iPr\ P)(CN)_2]^-Bu_4N^+$, however, the low field shift was again quite small, 2.76 ppm. In Figure 4 are given the ^1H NMR spectra of $[Fe(TEtP)(CN)_2]^-Bu_4N^+$ taken at −25 °C in CD_2Cl_2 and $CD_2Cl_2-CD_3OD$ as typical examples.

(ii) ^{13}C NMR Spectra. The cyanide carbon signal also moved to lower field by the addition of methanol. The results are listed in Table 2. As in the case of the pyrrole proton signals, the methanol effect on the ^{13}C chemical shifts was quite large in $[Fe(TMeP)(CN)_2]^-Bu_4N^+$ and $[Fe(TEtP)(CN)_2]^-Bu_4N^+$, 439 and 497 ppm, respectively. In contrast, the effect was much smaller in $[Fe(THP)(CN)_2]^-Bu_4N^+$ and $[Fe(T^iPrP)(CN)_2]^-Bu_4N^+$, 10 and 141 ppm, respectively. In Figure 5 are shown the ^{13}C NMR spectra of $[Fe(TEtP)(^{13}CN)_2]^-Bu_4N^+$ taken at −25 °C in CD_2Cl_2 and $CD_2Cl_2-CD_3OD$ solutions as typical examples.

(iii) EPR Spectra. The alkyl substituted complexes gave sharper signals in the presence of methanol. In Figure 6 are shown the EPR spectra of $[Fe(TEtP)(^{13}CN)_2]^-Bu_4N^+$ taken at 77 K in frozen CH_2Cl_2 and $CH_2Cl_2-CH_3OH$ solutions as typical examples. The *g* values were determined at 4.2 K by the computer simulation of the observed curve. In Figure 7 are given the observed and the simulated spectra of $[Fe(T^iPr\ P)(CN)_2]^-Bu_4N^+$ as a typical example. The *g* values thus determined are also listed in Table 3.

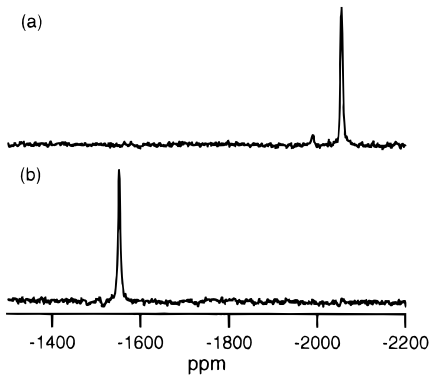

Figure 5. ^{13}C NMR spectra (156 MHz) of $[Fe(TEtP)(CN)_2]^-Bu_4N^+$ taken at −25 °C in (a) CD_2Cl_2 and (b) $CD_2Cl_2-CD_3OD$.

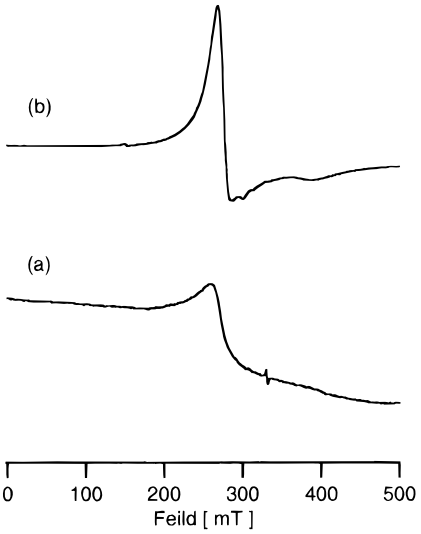

Figure 6. EPR spectra of $[Fe(TEtP)(CN)_2]^-Bu_4N^+$ taken at 77 K in (a) CH_2Cl_2 and (b) $CH_2Cl_2-CH_3OH$.

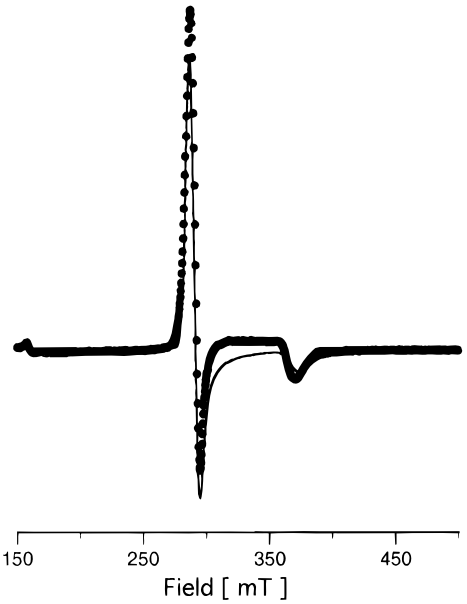

Figure 7. Simulation of the EPR spectrum of $[Fe(T^iPrP)(CN)_2]^-Bu_4N^+$ measured at 4.2 K in frozen $CH_2Cl_2-CH_3OH$ solution.

Discussion

^1H NMR and EPR Spectra. Most of the bis(cyanide) complexes reported previously gave spectroscopic features characteristic of low spin complexes. A typical example is $[Fe(TPP)(CN)_2]^-$, which showed a pyrrole β-signal at −16.4

ppm at 25 °C in ^{1}H NMR[14] and a large g_{max} signal at 3.70 in EPR spectrum.[47] The former was ascribed to the charge transfer from porphyrin ($3e_g$) to iron (d_π) orbitals, and the latter was interpreted as the near degeneracy of the d_{xz} and d_{yz} orbitals. Thus, the ground state electronic configuration of this complex was assigned to the usual $(d_{xy})^2(d_{xz}, d_{yz})^3$. Lukas and Silver[48] pointed out the possibility of the unusual $(d_{xz}, d_{yz})^4(d_{xy})^1$ configuration in [Fe(PP)(CN)$_2$]$^-$; PP is a dianion of protoporphyrin IX, based on the very small quadrupole splitting ΔE_q = 0.40 mm s^{-1} (25 °C) as compared with that of bis(imidazole) complex [Fe(PP)(Im)$_2$]$^-$ ΔE_q = 2.27 mm s^{-1} (25 °C)[49] in the Mossbauer spectra. The ^{1}H NMR and EPR spectra of the unsubstituted [Fe(T*H*P)(CN)$_2$]$^-$ are quite similar to those of the typical low spin ferric porphyrins in a sense that the complex showed a pyrrole signal at $\delta = -16.8$ ppm (25 °C) and a large g_{max} type EPR signal at 3.65. Thus, the electronic ground state of this complex should be assigned to the usual $(d_{xy})^2(d_{xz},d_{yz})^3$ with nearly degenerate d_{xz} and d_{yz} orbitals.

When the alkyl substituents are introduced at the *meso* positions, spectroscopic properties changed to a great extent as listed in Tables 1−3. A large low field shift of the pyrrole ^{1}H NMR signals together with the axial EPR spectra in these complexes strongly indicate that the ground state electron configuration is predominantly $(d_{xz}, d_{yz})^4(d_{xy})^1$. In Figure 8a is shown the variation of the absolute g values of the low-spin ferric porphyrin complexes having axial symmetry as rhombic splitting value Δ/λ varies.[50] The negative sign of Δ/λ indicates that d_{xy} is higher in energy than d_{xz} and d_{yz}. The energy gaps between d_{xy} and the degenerate d_{xz}, d_{yz} pair obtained from Figure 8a are summarized in Figure 8b. It should be noted that the energy levels are relative ones; the energy level of the d_{xz} and d_{yz} orbitals in Figure 8b is tentatively placed at the constant position which will be discussed later in this paper. The signs of the three g values were assumed to be $g_x = -g_y$ and $g_z < 0$ based on the Taylor's model.[51] By using the negative values for g_x and g_z and positive for g_y, we were able to calculate the coefficients a, b, and c of the wave functions for d_{xz}, d_{yz}, and d_{xy} orbitals. These values are also listed in Table 3. The coefficients suggest that the orbital of the unpaired electron has 96% d_{xy} character in the *Me*, 94% in the *Et*, and 98% in the ^{i}*Pr* complex. It is strange that the ratio is larger in the *Me* than in the *Et* complex even though ethyl is much bulkier than methyl group. Similar reversal was observed in the pyrrole ^{1}H chemical shifts; the chemical shift of the *Me* complex is lower than those of the *Et* complex. In the complex with pure $(d_{xz},d_{yz})^4(d_{xy})^1$ configuration, three g values are expected to be equal, $g_x = g_y = g_z = 2$. Thus, the ^{i}*Pr* complex [Fe(T^i*Pr*P)(CN)$_2$]$^-$Bu$_4$N$^+$ with g_x = 2.35, g_y = 2.35, g_z = 1.82 in $CH_2Cl_2-CH_3OH$ is quite close to the complex with pure $(d_{xz}, d_{yz})^4(d_{xy})^1$ configuration.[52] Corresponding to the EPR results, the pyrrole protons of the ^{i}*Pr* complex appeared at δ = 12.8 (−25 °C) in the presence of methanol. Taken together, the electronic configuration of [Fe(T*R*P)(CN)$_2$]$^-$ where *R* = *Me*, *Et*, and ^{i}*Pr*, is best presented as $(d_{xz}, d_{yz})^4(d_{xy})^1$.

^{13}C NMR Spectra. The electron configuration must be reflected to the ^{13}C chemical shifts of the coordinated cyanide since the carbon is directly bonded to the ferric ion. Various ferric porphyrin complexes with bis(cyanide) coordination have been examined by ^{13}C NMR. The chemical shifts were in the range of −2000 to −2400 ppm. The large isotropic shifts in these complexes must be ascribed to the iron (d_π)−cyanide (p_π) interactions in which iron has $(d_{xy})^2(d_{xz}, d_{yz})^3$ electron configuration. Since the d_{xy} orbital is orthogonal to the π and π^* orbitals of the coordinated cyanide, the change in electron configuration from $(d_{xy})^2(d_{xz},d_{yz})^3$ to $(d_{xz}, d_{yz})^4(d_{xy})^1$ would result in the decrease in the isotropic shift of the cyanide carbon signal. As expected, the data in Table 2 show a substantial decrease in the isotropic shifts in going from the unsubstituted complex to the ^{i}*Pr* complex; the difference in chemical shifts between [Fe(T*H*P)(CN)$_2$]$^-$ and [Fe(T^i*Pr*P)(CN)$_2$]$^-$ reached as much as 1574 ppm in $CD_2Cl_2-CD_3OD$ solution at −25 °C. This contrasts the results reported by Goff[53] in which chemical shifts of cyanide carbons are in the narrow range of 400 ppm in spite of the presence of electronically different substituents at the porphyrin periphery, supporting again the change in electronic configuration. Figure 9 shows the correlation of the chemical shifts between the pyrrole proton and cyanide carbon signals. A fairly good correlation suggests that the change in chemical shifts of the protons and carbons has the same origin. Curiously, the cyanide signal appeared still at a very high field in the complexes where the orbital of the unpaired electron has nearly

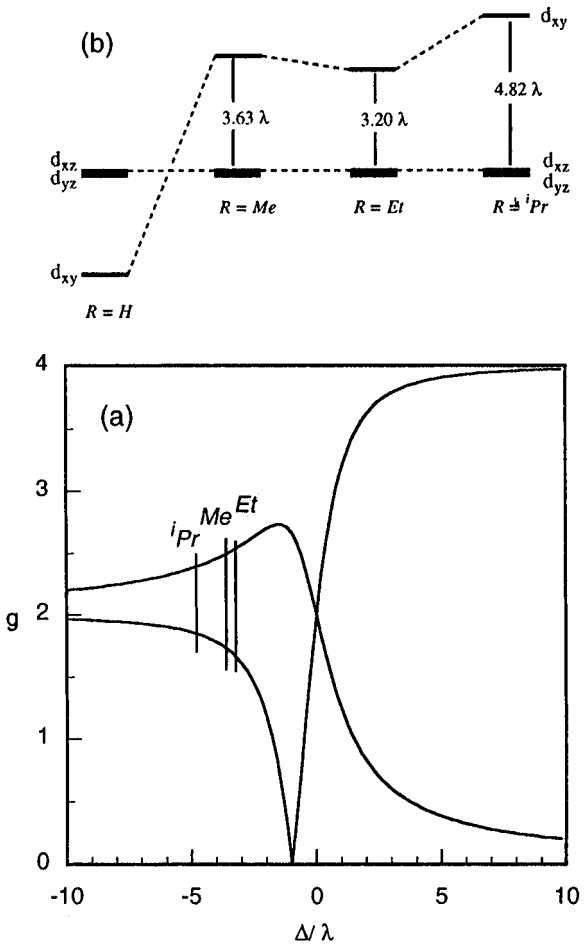

Figure 8. (a) Variation of the absolute g values of the low spin ferric porphyrin complexes having axial symmetry as rhombic splitting Δ/λ varies. (b) Relative energy levels of the three d orbitals in a series of [Fe(T*R*P)(CN)$_2$]$^-$Bu$_4$N$^+$ calculated based on the EPR results in frozen $CH_2Cl_2-CH_3OH$ solution at 4.2 K. The energy level of the d_{xy} orbital is tentatively placed at the constant position.

(47) Inniss, D.; Soltis, S. M.; Strouse, C. E. *J. Am. Chem. Soc.* **1988**, *110*, 5644−5650.
(48) Lukas, B.; Silver, J. *Inorg. Chim. Acta* **1986**, *124*, 97−100.
(49) Epstein, L. M.; Straub, D. K.; Maricondi, C. *Inorg. Chem.* **1967**, *6*, 1720.
(50) Bohan, T. L. *J. Magn. Reson.* **1977**, *22*, 109−118
(51) Taylor, C. P. S. *Biochim. Biophys. Acta* **1977**, *491*, 137−149.
(52) It was reported recently that the complexes with π-acid axial ligands, [Fe(TPP)(^{t}BuNC)$_2$]ClO$_4$ and [Fe(OEP)(^{t}BuNC)$_2$]ClO$_4$, show axial EPR spectra. The former complex shows $g_\perp$ = 2.21 and $g_\parallel$ = 1.93 in frozen CH_2Cl_2 solution at 77 K which corresponds to the 98% $(d_{xz},d_{yz})^4(d_{xy})^1$ character.[23]
(53) Goff, H. M. *J. Am. Chem. Soc.* **1977**, *99*, 7723−7725.

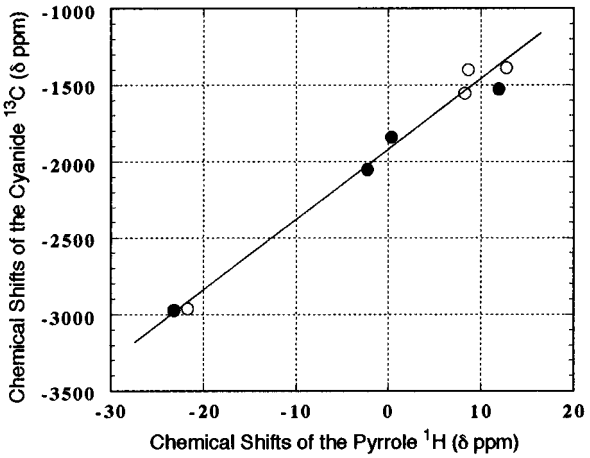

Figure 9. Correlation of the chemical shifts between pyrrole proton and cyanide carbon signals. Black circles are the chemical shifts in CD_2Cl_2 and white circles are those in $CD_2Cl_2-CD_3OD$.

98% d_{xy} character as revealed from the EPR results. The results suggest that the spin polarization gives rise to significant spin density on the CN carbon.

Reasons for the Unusual Electron Configuration. The important question arises as to why the electron configuration changes from the usual $(d_{xy})^2(d_{xz}, d_{yz})^3$ to the unusual $(d_{xz}, d_{yz})^4(d_{xy})^1$ as the bulkiness of the *meso* substituents increases. As was pointed out, $(d_{xz}, d_{yz})^4(d_{xy})^1$ ground state is stabilized if the axial ligands have weak σ donating and strong π accepting character.[17,20,21] In the present case, however, cyanide is a strong σ donor. In addition, stabilization of the iron d_π orbitals by the cyanide π^* is not important since unsubstituted complex showed quite normal spectroscopic properties. Inspection of the data in Tables 1 and 2 reveals that there is a large difference in chemical shifts between the unsubstituted and the *Me* complexes; the difference in pyrrole proton shifts is 23.53 ppm and that in cyanide carbon shifts is 1133 ppm in CD_2Cl_2.

Recently, systematic studies on the molecular structures of a series of nickel(II) *meso*-tetrasubstituted porphyrin complexes have been carried out by molecular mechanics calculation and in some cases by X-ray crystallographic analysis.[54] According to this study, the ruffling dihedral angle, defined by $C_\alpha N-NC_\alpha$ for nitrogens in opposite pyrroles, increases as the size of *meso* substituents increases; the angles in the *Me*, *Et*, and *^{i}Pr* complexes are calculated to be 25.3°, 21.0°, and 36.6°, respectively. It is noteworthy that the *Me* complex is slightly more deformed than the *Et* complex. Thus, the order of the ruffling dihedral angles, H << Et < Me << ^{i}Pr, is in good agreement with the order of the chemical shifts of the pyrrole protons and cyanide carbons as well as the EPR *g* values. This is the indication that the unusual electron configuration of $[Fe(TRP)(CN)_2]^-$ is caused by the nonplanarity of the porphyrin ring. Another characteristic feature in the deformed porphyrin rings is the contraction of the nickel−nitrogen (porphyrin) Ni−N_p bond distance; the calculation shows that the Ni−N_p bond decreases from 1.951 Å in the planar [Ni(TPP)] to 1.903 Å in the nonplanar [Ni(T*^{i}Pr*P)]. The same tendency is observed in the Fe−N_p bond in low spin ferric porphyrin complexes; the Fe−N_p bond decreases from 1.994 Å in the planar $[Fe(TPP)(HIm)_2]^+$ to 1.937 Å in the nonplanar $[Fe(TMP)(2\text{-}MeIm)_2]^+$.[55,56]

The contraction of the Fe−N_p bond in the deformed porphyrin system would destabilize not only $d_{x^2-y^2}$ orbital but also d_{xy} orbital due to the stronger σ donation of porphyrin nitrogens toward iron. The ruffled porphyrin core would also destabilize d_{xy} orbital due to the σ-type interaction with the porphyrin a_{2u} orbitals.[20] Another factor to be considered is the change in energy level of the $d_\pi(d_{xz}, d_{yz})$ orbitals as the porphyrin ring goes from the planar to the S_4 ruffled structure. While the strong $p_\pi-d_\pi$ interactions among porphyrin 3_{eg} and iron d_π orbitals are expected in a planar D_{4h} complex, the interaction would be weakened in an S_4 ruffled structure due to less overlap of the interacting orbitals, resulting in the lowering of the energy level of the d_π orbitals. Thus, in a strongly ruffled low spin complex such as $[Fe(T^iPr\ P)(L)_2]^\pm$, it is expected that the destabilization of the d_{xy} and/or stabilization of the d_π orbitals leads to the formation of $(d_{xz},d_{yz})^4(d_{xy})^1$ ground state configuration regardless of the kind and basicity of the axial ligands.

In order to test if this is correct, we measured the ^{1}H NMR and EPR spectra of $[Fe(T^iPr\ P)(Py)_2]+$, since pyridine(Py) is a typical ligand to form low spin complexes with the usual electron configuration. In fact, $[Fe(TMP)(Py)_2]^+$ gave a pyrrole signal at −13.3 ppm (−80 °C)[17] and $[Fe(TPP)(Py)_2]^+$ showed a g_{max} type EPR signal at 3.70.[47] As we have expected, the pyrrole signal of $[Fe(T^iPrP)(Py)_2]^+$ appeared at quite a low field, $\delta = +16.4$ ppm at −87 °C, which is actually the lowest pyrrole signal ever reported for the low spin ferric porphyrin complexes. Correspondingly, the EPR spectrum of this complex taken in frozen CH_2Cl_2 solution showed a clear axial type spectrum even at 77 K, $g_\perp = 2.46$ and $g_{||} = 1.59$. Existence of the low field pyrrole signals together with the axial EPR spectrum strongly suggests that the electron configuration is presented as $(d_{xz}, d_{yz})^4(d_{xy})^1$ even in $[Fe(T^iPr\ P)(Py)_2]^+$, supporting the hypothesis mentioned above.

In this study, we have shown that the S_4-ruffled porphyrin core is essential to the unusual $(d_{xz}, d_{yz})^4(d_{xy})^1$ electron configuration. Interestingly, recent crystallographic studies[20,23] of the complexes with the unusual $(d_{xz}, d_{yz})^4(d_{xy})^1$ configuration such as $[Fe(TPP)(4\text{-}CNPy)_2]^+$, $[Fe(TPP)(^tBuNC)_2]^+$, and $[Fe(TPP)\{(P(OMe)_2Ph\}]^+$ also revealed a strongly S_4-ruffled structure in spite of the fact that the porphyrin core in TPP generally shows planar or slightly deformed structure.[47,57−59] These results suggest that the porphyrin distortion is correlated with the relative stability of the two states, $(d_{xz}, d_{yz})^4(d_{xy})^1$ and $(d_{xy})^2(d_{xz}, d_{yz})^4$. In the present case, distortion of porphyrin caused by *meso* substitution causes destabilization of d_{xy} orbital and/or stabilization of d_{xz}, d_{yz} orbitals, resulting in the unusual $(d_{xz}, d_{yz})^4(d_{xy})^1$ electron configuration. On the other hand, the unusual $(d_{xz}, d_{yz})^4(d_{xy})^1$ electron configuration in the previous cases was caused by the donor properties of the axial ligands. When the axial ligands with fairly weak ligand field such as 4-CNPy, ^{t}BuNC, and $P(OMe)_2Ph$ coordinate to the ferric porphyrin to form the low spin complexes, the d_{xz} and d_{yz} orbitals would be stabilized both by the weak σ-donation and by the interaction with low lying π^* orbitals of the axial ligand.[17,20,21] This may lead to the unusual $(d_{xz}, d_{yz})^4(d_{xy})^1$ electron configuration where the d_{xy} is slightly higher in energy than the d_{xz} and d_{yz}. However, the electronic state in which three d orbitals are energetically close is supposed to be unfavorable in total energy. Thus, the porphyrin core could be

(54) Jentzen, W.; Simpson, M. C.; Hobbs, J. D.; Song, X.; Ema, T.; Nelson, N. Y.; Medforth, C. J.; Smith, K. M.; Veyrat, M.; Mazzanti, M.; Ramasseul, R.; Marchon, J. C.; Takeuchi, T.; Goddard III, W. A.; Shelnutt, J. A. *J. Am. Chem. Soc.* **1995**, *117*, 11085−11097.

(55) Walker, F. A.; Huynh, B. H.; Scheidt, W. R.; Osvath, S. R. *J. Am. Chem. Soc.* **1986**, *108*, 5288.

(56) Munro, O. Q.; Marques, H. M.; Debrunner, P. G.; Mohanrao, K.; Scheidt, W. R. *J. Am. Chem. Soc.* **1995**, *117*, 935−954.

(57) Quinn, R.; Valentine, J. S.; Byrn, M. P.; Strouse, C. E. *J. Am. Chem. Soc.* **1987**, *109*, 3301−3308.

(58) Schappacher, M.; Fischer, J.; Weiss, R. *Inorg. Chem.* **1989**, *28*, 389−392.

(59) Higgins, T. B.; Safo, M. K.; Scheidt, W. R. *Inorg. Chim. Acta.* **1990**, *178*, 261−267.

S_4-ruffled, relieving the nearly degenerated states and lowering the total energy by flipping the d_{xy} orbital energy up.

Methanol Effects. We found that the ^{1}H and ^{13}C chemical shifts as well as the signal width in EPR spectra are greatly affected by the addition of methanol. As the data in Tables 1 and 2 indicate, the addition of methanol induced large low field shifts of both pyrrole proton and cyanide carbon signals. Coordinated cyanide is known to have a proton acceptor ability.[14,60] Thus, the hydrogen bonding with methanol decreases the σ basicity and increases the π acceptor properties. This will increase the energy gap between d_{xy} and (d_{xz}, d_{yz}) orbitals in $(d_{xz}, d_{yz})^4(d_{xy})^1$ ground state configuration, resulting in the low field shift of the pyrrole proton and cyanide carbon signals. As mentioned, the methanol effect is larger in the *Me* and *Et* complexes than in the *H* and *^{i}Pr* complexes. This can also be explained by considering the energy gap between d_{xy} and (d_{xz}, d_{yz}) orbitals. In the case of the *^{i}Pr* complex, the energy gap is already fairly large in CD_2Cl_2 solution due to the strongly ruffled porphyrin structure. As a result, lowering of the (d_{xz}, d_{yz}) orbitals does not cause significant effects on the chemical shifts; low field shifts were 0.82 and 141 ppm for the ^{1}H and ^{13}C signals, respectively. In the case of the unsubstituted complex, orbital ground state configuration places d_{xz}, d_{yz} above d_{xy}. Although the hydrogen bonding lowers the energy levels of d_{xz} and d_{yz} orbitals, the energy levels of these orbitals are expected to be still higher than that of d_{xy} orbital because of the planarity of the porphyrin ring. As a result, the low field shifts in ^{1}H and ^{13}C signals were rather small, 1.46 and 10 ppm, respectively. In the intermediate case, the *Me* and *Et* complexes, the energy gap between d_{xy} and (d_{xz}, d_{yz}) is much smaller than that in the *^{i}Pr* complex. Thus, the stabilization of the d_{xz} and d_{yz} orbitals by the hydrogen bond greatly affects the ^{1}H and ^{13}C NMR chemical shifts.

Acknowledgment. We thank Professor Saburo Neya of Kyoto Pharmaceutical University for various information on the synthesis of tetraalkylporphyrins. This work was supported by a Grant in Aid for Scientific Research (No. 07640732) from Ministry of Education, Science and Culture of Japan.

JA970602R

(60) Morishima, I.; Inubushi, T. *J. Am. Chem. Soc.* **1978**, *100*, 3568−3574.